TECHNICAL NOTE

D-103

INVESTIGATION OF DOUBLE SLOTTED FLAPS ON A

SWEPT-WING TRANSPORT MODEL

By Rodger L. Naeseth and Edwin E. Davenport

Langley Research Center
Langley Field, Va.

NATIONAL AERONAUTICS AND SPACE ADMINISTRATION

WASHINGTON   October 1959

NATIONAL AERONAUTICS AND SPACE ADMINISTRATIon

TECHNICAL NOTE D-103

INVESTIGATION OF DOUBLE SLOTTED FLAPS ON A

SWEPT-WING TRANSPORT MODEL

By Rodger L. Naeseth and Edwin E. Davenport

SUMMARY

A low-speed wind-tunnel investigation has been made at a Reynolds number of 0.9×10^6 to determine the longitudinal aerodynamic character- istics of a double slotted flap on a wing swept back 35° at the quarter chord. The wing had an aspect ratio of 7 and a taper ratio of 0.3. The flap was 0.33 wing chord and the vane was 0.50 flap chord.

A maximum lift coefficient of 2.2 was obtained with the double slotted flap in conjunction with a leading-edge slat. The lift coeffi- cient increment at $\alpha = 0^\circ$ and $\delta_f = 70.7^\circ$ was 1.43. This value was predicted by a method presented in NACA Technical Note 3911.

The method of design of the flap was based largely on two- dimensional double-slotted-flap results. Changes to the geometry of the flap indicated only small improvements in lift characteristics. Also, alterations which involved sealing one or both slots resulted in losses in lift and increases in drag at high lift coefficient.

Large diving moments were encountered which would have required a tail download for trim amounting to a lift-coefficient increment of as much as 0.17. This analysis assumes a tail length of three mean aero- dynamic chords and a center of gravity located at 0.3 mean aerodynamic chord, which are typical characteristics of present swept-wing trans- port designs.

INTRODUCTION

Consideration of the landing and take-off problems of current transport designs has shown a need for improved high-lift devices. The problem is critical because of the combination of high wing loading, wing sweepback, and jet powerplants. In order to keep take-off velocity reasonable with increased wing loading, it is necessary to increase the maximum lift coefficient; however, wing sweepback tends to reduce maximum

lift coefficient and also the effectiveness of high-lift devices. The use of jet powerplants means that the lift resulting from the increase in slipstream velocity over the wing behind the propellers can no longer be counted on as an operational margin in landing and take-off maneuvers (ref. 1). To meet the need for effective high-lift devices on wings of moderate sweep and aspect ratio, an investigation has been made at the Ames and the Langley Research Centers to design and test a double slotted flap through a large Reynolds number range. The results of the Ames tests are given in reference 2. The present report covers the design and the small-scale tests.

The gain in lift produced by a double slotted flap as compared to a plain flap is due to the increased area of the double slotted flap and to the increased flap-deflection angle which can be attained. The increase in flap-deflection angle before a loss in flap effectiveness occurs is possible because of the boundary-layer control over the flap due to the flow of air through the slots. Because of this characteristic, the use of slots can be considered a form of boundary-layer control along with suction and blowing.

Results of reference 3 indicate that for a blowing flap the momentum coefficient to obtain a given lift coefficient was minimum for a ratio of flap chord to wing chord of $1/3$. Also, it was shown in this reference that a ratio of vane chord to flap chord of $1/2$ was a good design value. In the present investigation these ratios were used to design the double slotted flap for a wing-fuselage combination representative of a current transport.

The present report presents the results of tests to determine the longitudinal aerodynamic characteristics of the wing-fuselage combination equipped with double slotted flaps of 0.537 semispan and which could be retracted into the space rearward of the 0.6-wing-chord line. The effects of leading-edge slats, engine nacelles, and some modifications to the slot design were determined.

The wing used in this investigation was swept back $35°$ at the quarter chord, had an aspect ratio of 7 and a taper ratio of 0.3, and was tapered in thickness ratio from 0.14c at the root to 0.10c at the tip. Airfoil sections were NACA $65_{(015)}A414$ and $65A410$, in the streamwise direction at the root and tip, respectively. The tests were made in the Langley 300-MPH 7- by 10-foot tunnel.

SYMBOLS

The forces and moments measured on the wing are presented about the wind axes which, for the conditions of these tests (zero sideslip),

correspond to the stability axes. The pitching-moment data are measured about the origin of axes, as shown in figure 1, which is a point $0.3\bar{c}$ rearward of the leading edge of $\bar{c}$ and $0.223\bar{c}$ above the wing-chord plane. The lift, drag, and pitching-moment data presented herein represent the aerodynamic effects of deflection of the flaps in the same direction on both semispans of the complete wing.

b	wing span, ft
C_D	drag coefficient, $\dfrac{\text{Drag}}{qS}$
C_L	lift coefficient, $\dfrac{\text{Lift}}{qS}$
C_m	pitching-moment coefficient, $\dfrac{\text{Pitching moment}}{qS\bar{c}}$
c	local chord, ft
$\bar{c}$	mean aerodynamic chord of wing, ft
c_f	flap chord, ft
q	free-stream dynamic pressure, $\dfrac{\rho V^2}{2}$, lb/sq ft
R	Reynolds number
S	wing area, sq ft
V	free-stream velocity, ft/sec
α	angle of attack of wing, deg
δ_f	flap deflection relative to wing chord plane, measured normal to 0.812-wing-chord line (positive when trailing edge is down), deg
ρ	mass density of air, slugs/cu ft

APPARATUS AND MODEL

A sketch and a photograph of the semispan model are given as figures 1 and 2, respectively. The wing had an aspect ratio of 7, a taper

ratio of 0.3, and was swept back 35° at the quarter-chord line. The air-
foil sections (streamwise) were tapered linearly in thickness ratio from
an NACA $65_{(015)}A414$ section at the root to a 65A410 section at the tip.
The wing was mounted on the fuselage in a low position and with zero
incidence and dihedral.

The wing was fitted with nacelles (figs. 1 and 3) designed by the
Ames Research Center staff. Faired nose inlet plugs were provided to
stop the internal flow in the nacelles.

Details of the leading-edge-slat configurations are shown in fig-
ure 4. Slat 1 had a St. Cyr 156 section and extended from 0.385b/2 to
0.970b/2. Slat 2 (ordinates are given in table I) extended from
0.442b/2 to 0.649b/2 and from 0.708b/2 to 0.915b/2. Slat 2a was slat 2
with the portion extending from 0.442b/2 to 0.649b/2 removed.

The double slotted flaps were designed to retract into a space
(fig. 1) which extended from 0.089b/2 to 0.626b/2 in the spanwise direc-
tion and included all that part of the wing behind the 0.60-wing-chord
line. The chord of the main flap of the double slotted flap was chosen
as 0.333c, and the chord of the vane as one-half of the flap chord. A
sketch of the flap in combination with the vane is given in figure 5 and
details of the airfoil sections and flap-vane assembly are given in
table II. The main flap airfoil sections are given along the ends of
the flap with the flap in the retracted position and hence are stream-
wise lines (table II). The vane plan form was laid out with the vane
chord line at zero angle of attack and with the vane located at the
pivot point. The vane sections are given along the ends of the vane in
this location and are streamwise. Details of the flap-vane assembly
are given in table II. Reductions of about one-half in the flap-vane
slot size were made either by taping a thin metal strip to the vane
trailing edge (fig. 5) or by moving the main flap forward on the sup-
porting brackets.

The wing was a steel box covered with mahogany. The flap was made
of mahogany reinforced with an aluminum plate which extended to the
trailing edge. The vane was machined from aluminum.

The semispan model was mounted vertically in the Langley 300-MPH
7- by 10-foot tunnel on the mechanical balance. The root chord of the
model was adjacent to the ceiling of the tunnel, which served as a
reflection plane. A small clearance was maintained between the model
and the tunnel ceiling so that no part of the model came in contact
with the tunnel structure. The fuselage minimized the effect of span-
wise air flow over the model through this clearance hole.

TESTS AND CORRECTIONS

Description of Tests

All tests were made in the Langley 300-MPH 7- by 10-foot tunnel. Data were obtained through an angle-of-attack range from -8° to 14° for all configurations. The flap-deflection range was from 41.0° to 80.4°.

The tests were performed at an average dynamic pressure of 24.8 pounds per square foot, which corresponds to a Mach number of 0.13 and a Reynolds number of 0.9×10^6 based on the mean aerodynamic chord of the wing.

All tests were made with a fuselage but no tail. The test configurations and the figure on which the results are plotted are given in table III.

Corrections

Jet-boundary corrections, determined by the method presented in reference 4, have been applied to the angle of attack and to the drag-coefficient values. Blocking corrections, to account for the constriction effects of the model and its wake, have also been applied to the test data by the method of reference 5.

RESULTS AND DISCUSSION

Flap-Design Considerations

The basis for the choice of the ratios of flap chord to wing chord and of vane chord to flap chord used was discussed in the introduction. Once these values are chosen, there still remains the problem of detail design of the flap. A considerable amount of two-dimensional data have been obtained in which the flap-vane-wing relationship was systematically varied over a wide range. Such systematic three-dimensional tests are difficult from a model design standpoint. Therefore, some rules may be helpful in laying out a flap that will give good lift increments. The vane airfoil section should have a high angle of attack for stall and should have a rounded nose so that one pivot point will be sufficient to preserve a good vane-to-lip geometry through a large flap-deflection range. The vane can then be placed with leading edge at the same wing station as the upper lip and a slot of about 4 percent flap chord. Because a double slotted flap is designed primarily for use at high

deflection angles, the vane is set relative to the main flap to work efficiently as a lifting surface and a turning vane with the main flap at a large deflection. An angle of 25° has been successfully used. In addition, the vane and flap are positioned to give a slightly converging slot and so that a line extending the upper surface of the vane would intersect the flap forward of maximum thickness. The results are presented in the following sections for tests of the flap designed in this way and of some modifications to the design.

Presentation of Results

The longitudinal characteristics of the wing-fuselage combination are given in figure 6 for several flap deflections. The effect of flap deflections and the effect of the various leading-edge slat configurations are given in figures 7 to 10. A comparison showing the effect of adding the nacelles, open or plugged, is given in figure 11 for $\delta_f = 0^{\circ}$ and in figure 12 for $\delta_f = 70.7^{\circ}$. The effect of alterations to the slot configuration is shown in figures 13 to 15. A summary of the lift characteristics as a function of flap deflection is given in figure 16. Table III lists the configurations tested and the figure on which the results are plotted.

Lift Characteristics

Model with double slotted flaps.- The results of the basic wing-fuselage combination (fig. 6) indicate that a large lift increment was produced by deflection of the double slotted flaps. A loss in effectiveness is shown at about 75° flap deflection and $\alpha = 0^{\circ}$. (See also fig. 16(a).)

The flap-lift-coefficient increment was computed by means of reference 6 to be 1.4 for a value of δ_f of 70.7° which is a good approximation of the experimental results of 1.43 at $\alpha = 0^{\circ}$. The two-dimensional lift increment used in the computations by the method of reference 6 was obtained from the data of reference 3. The experimental two-dimensional lift increment of reference 3 for a flap-chord ratio of 0.25 was multiplied by the ratio of flap effectiveness parameter for a flap-chord ratio of 0.33 to that for 0.25 flap-chord ratio obtained from reference 6.

Maximum lift was limited by a progressively earlier stall as δ_f was increased. The leading-edge slat arrangements shown in figure 4 were used to delay stall (figs. 7 to 10). The values of C_L at $\alpha = 0^{\circ}$ and maximum lift coefficient $C_{L_{max}}$ are given as a function

of δ_f in figure 16(a). The maximum lift was increased from 1.92 to about 2.20 when slat 1 and the engine nacelles were installed on the wing (figs. 7 and 16(a)). Slat 2 (figs. 8, 9, and 16(a)) gave about the same increment of lift at $\alpha = 0^\circ$, but about 0.1 less in maximum lift. The outboard part of slat 2 alone (slat 2a) was ineffective (fig. 10). Note that, because the nacelles were open for tests of slat 1 and were plugged for tests of slat 2, the previous comparison of the results for slat 1 and slat 2 is valid only if the effects of plugging the nacelles are negligible, as is shown.

These nacelle-plugged tests were made to assess the performance effects of the internal flow. Figures 11 and 12 show that the effect of plugging the nacelles on lift was negligible for flap deflections of 0° and 70.7°. These data also show that the effect of adding the nacelles to the wing-fuselage combination increased maximum lift about 0.04 and had little or no effect when the flap was deflected.

Effect of various slot configurations.- Although the flap as originally designed gave satisfactory lift increments, some variations in the slots were made. The effects of sealing either or both of the slots at $\delta_f = 70.7^\circ$ are shown in figure 13. Sealing both gaps caused a loss in lift increment at $\alpha = 0^\circ$ of 0.46 and in maximum lift of 0.44. The results show that it is not possible to add up the separate effects of the slots to obtain the double-slotted-flap values. When the front slot only was opened there was a loss in lift at low angles of attack compared to the slots-closed condition, but the slot was effective at higher angles of attack which resulted in a maximum lift coefficient 0.16 greater for the slot-opened condition than for the slot-closed condition. With only the rear slot opened, the lift was the same as the double-slotted-flap value at $\alpha = -7^\circ$, but maximum lift coefficient was 1.90, the same as with only the front slot open.

An extension of the vane chord rearward or moving the flap forward with resultant decrease in vane to flap slot of about one-half gave improvement in lift. (Compare figs. 14 and 15 with fig. 12.) These results are compared in figure 16(b) at $\alpha = 0^\circ$ and at maximum C_L. The vane extension resulted in a 0.14 increase in lift coefficient at $\alpha = 0^\circ$ and a 0.06 increase in maximum lift coefficient for flap deflections to about 70°. It should be noted that this larger vane could not be stowed in the retracted position in the space rearward of the wing 0.6-chord line.

A slight gain in lift at $\alpha = 0^\circ$ and no gain in maximum lift resulted from moving the flap forward (figs. 15 and 16(b)). The results indicate that the design of the flaps can be improved by decreasing the gap some and by choosing a larger ratio of vane chord to flap chord.

Pitching-Moment Characteristics

The results for the plain wing and fuselage (fig. 6) show some stability up to $C_L = 0.5$ where a sharp pitchup tendency is shown. Adding slat 1 to the wing with flap zero (fig. 11) resulted in an unstable pitching-moment curve, which, however, did not exhibit any pitchup tendency until $C_{L_{max}} = 1.4$ was reached.

With the flaps deflected (fig. 7) the results show the large negative pitching moments usually characteristic of double slotted flaps. Based on a tail length of $3\bar{c}$ and a center-of-gravity position at $0.3\bar{c}$, which is typical of present swept-wing transport designs, the download required to trim $\left(C_m = -0.5\right)$ could amount to an incremental loss in C_L of 0.17.

Drag Characteristics

Minimum drag for the wing-fuselage combination was 0.014 (fig. 6(b)). Adding the nacelles (fig. 11(b)) increased the minimum drag to 0.020. The adding of leading-edge slat 1 (fig. 11(b)) caused further increase in minimum drag to 0.025.

The drag curves for the double slotted flaps typically appear less rounded than would be expected for a plain flap and thus show a possibly higher drag in the intermediate lift range and a lower drag in the high lift range. Figure 13 shows considerably lower drag at a given lift coefficient for the double slotted flap than for one or both slots sealed. The untrimmed lift-drag ratio was maximum for the wing-fuselage combination with flaps at the lowest deflection tested and was about 6.0.

Effect of Reynolds Number

The results of figure 6 for $\delta_f = 51^O$ are compared in figure 17 with the results of a similar configuration of reference 2. Although the configurations are reasonably the same, some differences in model and test technique existed. The tests of reference 2 were made on a complete model mounted on three struts, also the wing had 2^O incidence and 6° dihedral.

The effects of increasing Reynolds number on the lift and drag characteristics are about as expected. The lift curve shows some increase in slope, a sharper stall, and a substantial gain in maximum lift. These effects of Reynolds number agree with the trends of reference 2. For example, in reference 2, tail-on tests were made over a

range of higher Reynolds numbers, 2.8, 4.8, 6.2, and 8.1 × 10^6. These results showed little difference for the three highest Reynolds numbers. However, decreasing the Reynolds number from 4.8 to 2.8 × 10^6 resulted in a decrease in lift-curve slope and maximum lift.

Trends of pitching-moment-coefficient variation with Reynolds number shown in figure 15(b) of reference 2 for the configuration with nacelles and pylons removed are similar to the trends of figure 17.

CONCLUDING REMARKS

A low-speed wind-tunnel investigation of a semispan model has been made at a Reynolds number of 0.9 × 10^6 to determine the longitudinal aerodynamic characteristics of a double slotted flap on a wing swept back 35° at the quarter chord. The wing had an aspect ratio of 7 and a taper ratio of 0.3. The flap was 0.33 wing chord and the vane was 0.50 flap chord. The model had a fuselage and engine nacelles.

A maximum lift coefficient of 2.2 was obtained with the double slotted flap in conjunction with a leading-edge slat. The lift-coefficient increment at α = 0° and a flap deflection of 70.7° was 1.43. This value was predicted by a method presented in NACA Technical Note 3911.

The method of design of the flap was based largely on two-dimensional double-slotted-flap results. Changes to the geometry of the flap indicated only small improvements in lift characteristics. Also, alterations which involved sealing one or both slots resulted in losses in lift and increases in drag at high lift coefficient.

Large diving moments were encountered which would have required a tail download for trim amounting to a lift-coefficient increment of as much as 0.17. This analysis assumes a tail length of three mean aerodynamic chords and a center of gravity located at the 0.3 mean aerodynamic chord, which are typical characteristics of present swept-wing transport designs.

Langley Research Center,
    National Aeronautics and Space Administration,
        Langley Field, Va., July 16, 1959.
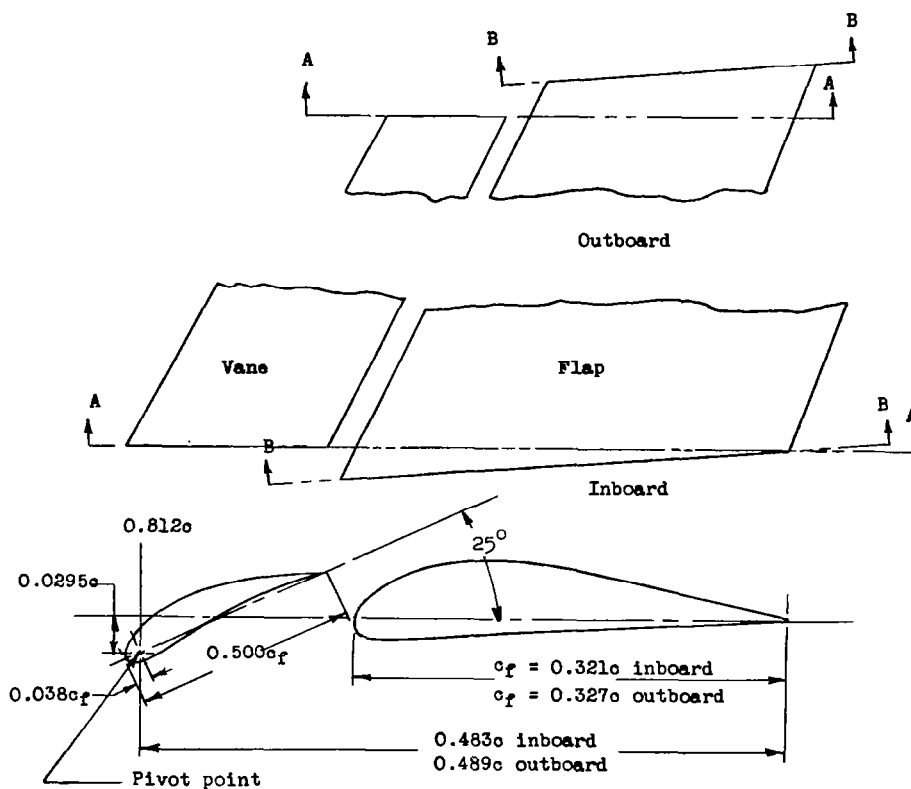
REFERENCES

1. Riebe, John M.: Consideration of Some Aerodynamic Characteristics During Take-Off and Landing of Jet Airplanes. NASA TN D-19, 1959.

2. Hickey, David H., and Aoyagi, Kiyoshi: Large-Scale Wind-Tunnel Tests of a Jet-Transport-Type Model With Leading- and Trailing-Edge High-Lift Devices. NACA RM A58H12, 1958.

3. Riebe, John M.: A Correlation of Two-Dimensional Data on Lift Coefficient Available With Blowing-, Suction-, Slotted-, and Plain-Flap High-Lift Devices. NACA RM L55D29a, 1955.

4. Polhamus, Edward C.: Jet-Boundary-Induced-Upwash Velocities for Swept Reflection-Plane Models Mounted Vertically in 7- by 10-Foot, Closed, Rectangular Wind Tunnels. NACA TN 1752, 1948.

5. Herriot, John G.: Blockage Corrections for Three-Dimensional-Flow Closed-Throat Wind Tunnels, With Consideration of the Effect of Compressibility. NACA Rep. 995, 1950. (Supersedes NACA RM A7B28.)

6. Lowry, John G., and Polhamus, Edward C.: A Method for Predicting Lift Increments Due to Flap Deflection at Low Angles of Attack in Incompressible Flow. NACA TN 3911, 1957.

TABLE I.- AIRFOIL ORDINATES FOR SLAT 2
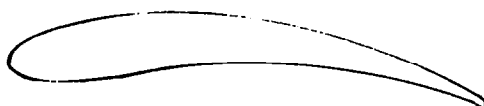
Station	Ordinate, percent chord	
	Upper	Lower
0	0	0
1.7	2.1	-2.6
3.3	3.2	-3.7
6.7	4.8	-4.9
13.3	7.1	-5.7
20.0	9.0	-5.2
26.7	10.2	-3.7
33.3	10.7	-2.0
40.0	10.6	-.9
46.7	10.1	-.5
53.0	9.1	-1.0
60.0	7.5	-1.5
66.7	5.9	-2.5
73.0	3.2	-3.1
80.0	.6	-5.1
86.7	-2.3	-6.7
93.0	-5.8	-8.2
100.0	-10.2	-10.2

TABLE II.- FLAP AIRFOIL SECTIONS AND DETAILS OF ASSEMBLY

Outboard

Vane   Flap

Inboard

0.812c

0.0295c

25°

0.500c_f

$c_f = 0.321c$ inboard
$c_f = 0.327c$ outboard

0.038c_f

0.483c inboard
0.489c outboard

Pivot point

Section A-A   Inboard and outboard

| Station | Vane (plane of section A-A) | | Flap (plane of section B-B) | | | |
| | Inboard and outboard | | Inboard | | Outboard | |
	Upper	Lower	Upper	Lower	Upper	Lower
0	0	0	-2.73	-2.73	-1.06	-1.06
1.25	3.81	-2.68	0.80	-5.33	2.52	-4.01
2.50	5.22	-3.39	2.80	-6.08	4.16	-4.77
5	7.39	-4.09	5.88	-6.51	6.59	-5.31
7.5	9.05	-4.46	8.15	-6.59	8.38	-5.47
10	10.50	-4.80	9.90	-6.59	9.84	-5.47
15	12.69	-4.09	12.48	-6.39	12.00	-5.22
20	14.40	-3.0	14.12	-5.93	13.39	-4.86
30	16.30	-1.40	15.28	-4.89	14.30	-4.01
40	16.60	0.1	14.92	-3.95	13.91	-3.16
50	16.00	1.8	12.75	-3.20	12.00	-2.58
60	14.40	3.0	10.26	-2.55	9.69	-2.06
70	11.70	3.2	7.75	-1.87	7.41	-1.52
80	8.30	2.0	5.19	-1.29	4.98	-1.03
90	4.50	1.8	2.66	-0.69	2.55	-0.58
95	2.60	1.07	1.35	-0.40	1.34	-0.33
100	0	0	0.09	-0.09	0.06	-0.06

TABLE III.- TEST CONFIGURATIONS AND FIGURES

ON WHICH DATA ARE PLOTTED

| Configuration | | | | | Figure | | | | | | | | |
| Slat | | | Nacelle | | | | | | | | | | |
1	2	2a(a)	Open	Plugged	$\delta_f = 0°$	41°	51°	55.9°	60.8°	66°	70.7°	75.5°	80.4°
(a) Double slotted flaps													
	Off		Off	Off	6,11	6	6		6		6,12	6	
	Off		X		11						12		
	Off			X	11						12	9	
	X			X					8,10		8,12	8,9	8
		X		X					10				
X			X		7,11		7		7	7	7,12,13	7	
(b) Both slots sealed													
X			X								13		
(c) Rearward slot sealed													
X			X								13		
(d) Forward slot sealed													
X			X								13		
(e) Trailing edge of vane extended to reduce slot													
X			X					14	14	14	14	14	

(f) Main flap moved forward to reduce slot

| Configuration | | | | | Figure | | | |
| Slat | | | Nacelle | | | | | |
1	2	2a(a)	Open	Plugged	$\delta_f = 55.9°$	61.5°	66.4°	71.6°
X			X		15	15	15	15

[a] Inboard part off; outboard part on.

Wing
Sweep of $\bar{c}/4$ .... 35°
Aspect ratio 7
Taper ratio 0.3
Twist .... 0°
Dihedral .... 0°
Area of semispan, ft 3.2
Airfoil section
Root .... NACA 65$_{(015)}$ A414
Tip .... NACA 65A410

.600 chord line,
wing cut out

.667 chord line,
nose of flap

←5.274→

$\frac{b}{2}$ =40.30

.700 $\frac{b}{2}$

.400 $\frac{b}{2}$

$\bar{c}$ =12.53

0.626 $\frac{b}{2}$

16.55

.089 $\frac{b}{2}$

2.80

Fuselage ⊄,
orgin of axes

18.92

16.61

17.58

.3 $\bar{c}$, orgin of axes

75.70
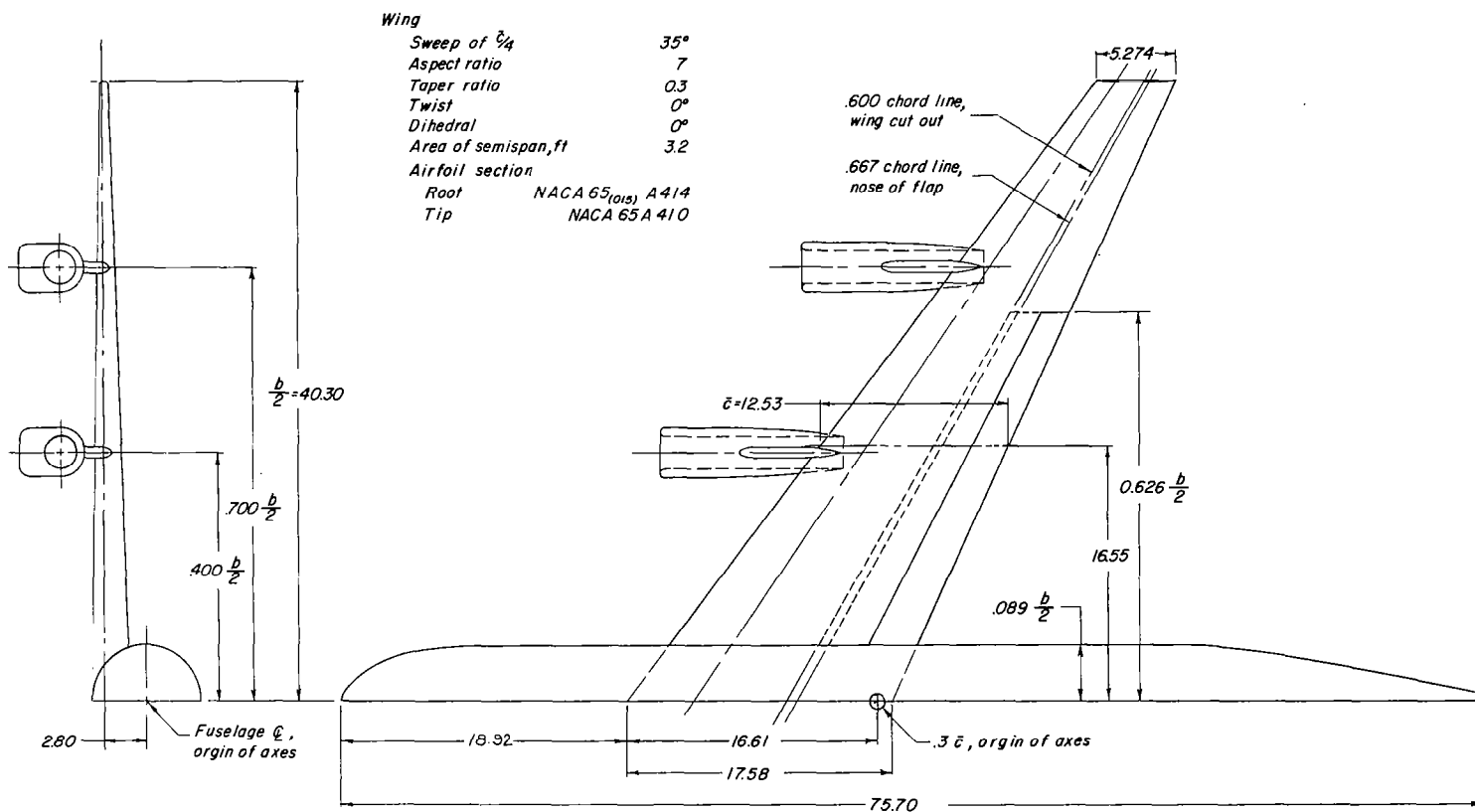
Figure 1.- Semispan model. All dimensions are in inches except as noted.
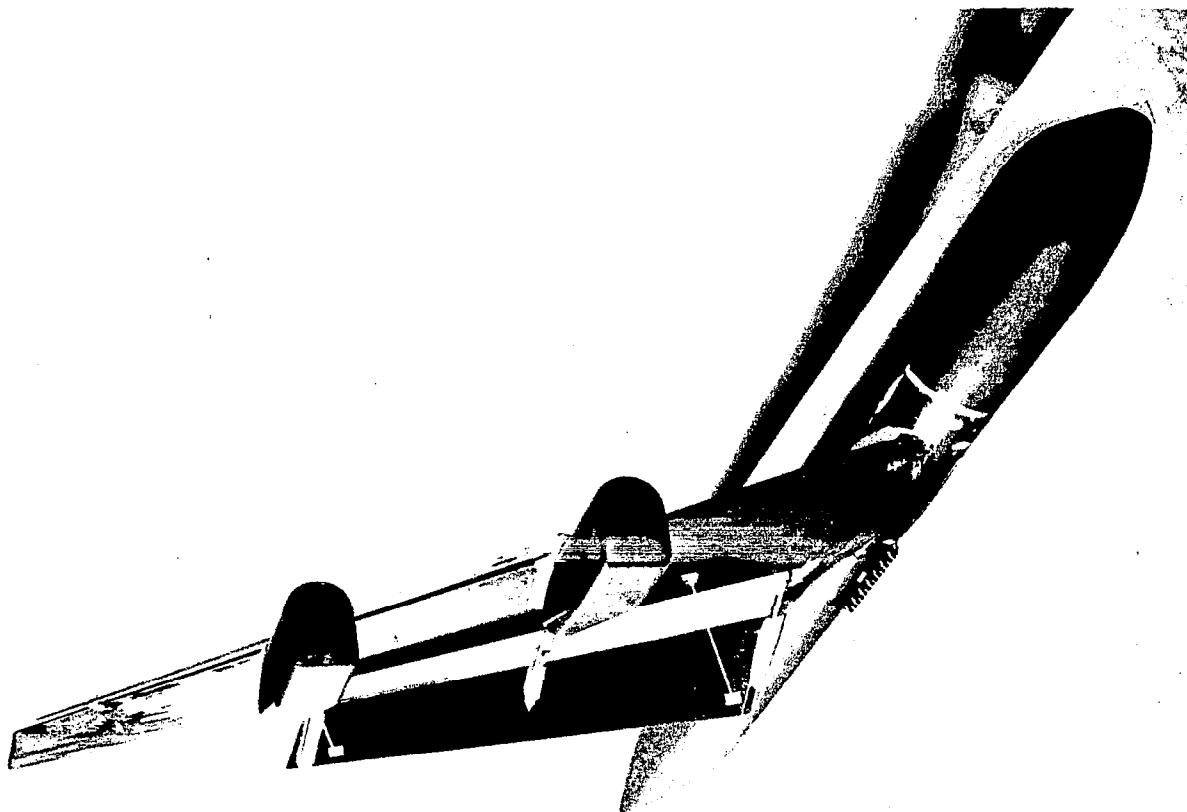
Figure 2.- Photograph of the semispan model.   L-58-1983
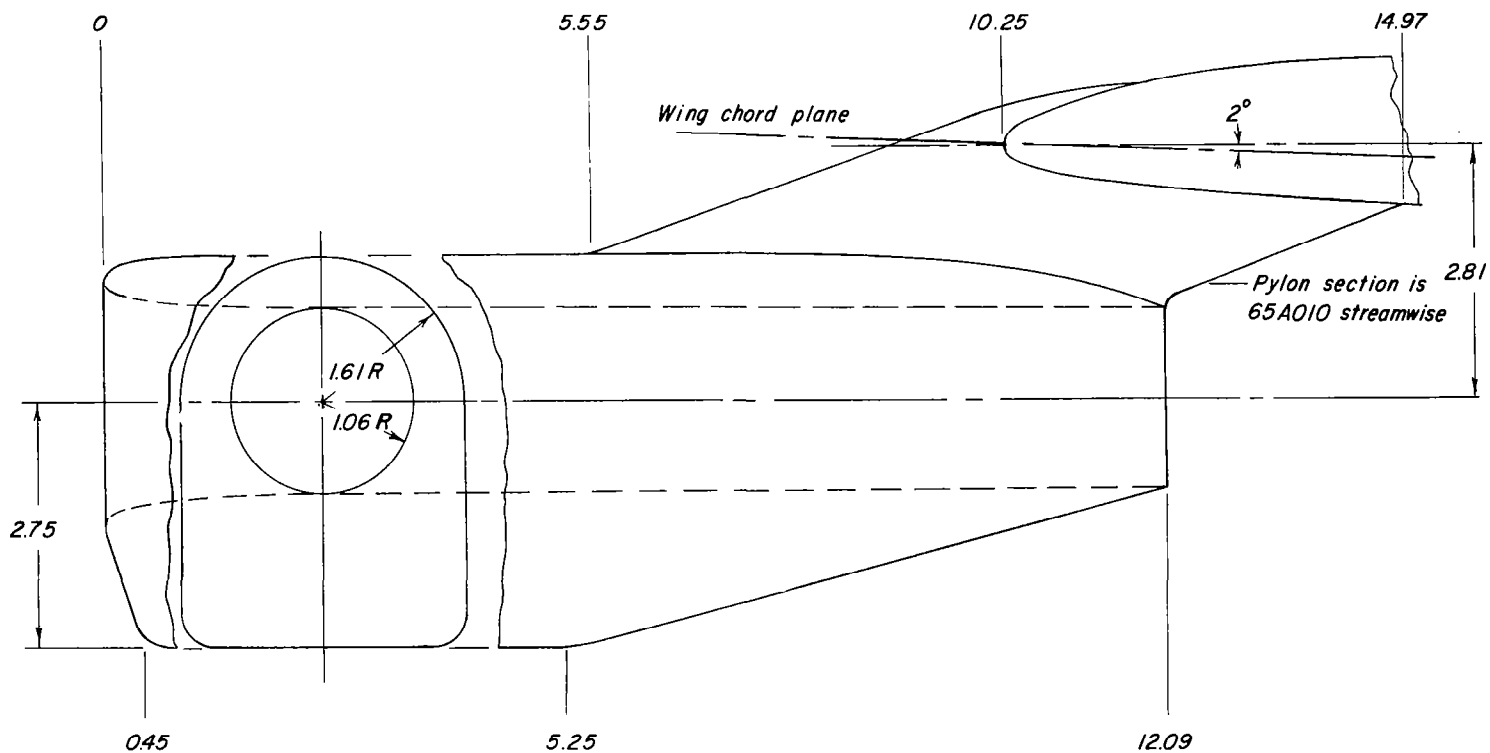
Figure 3.- Nacelle details. Dimensions are in inches.

(a) Slat 1.

(b) Slat 2.
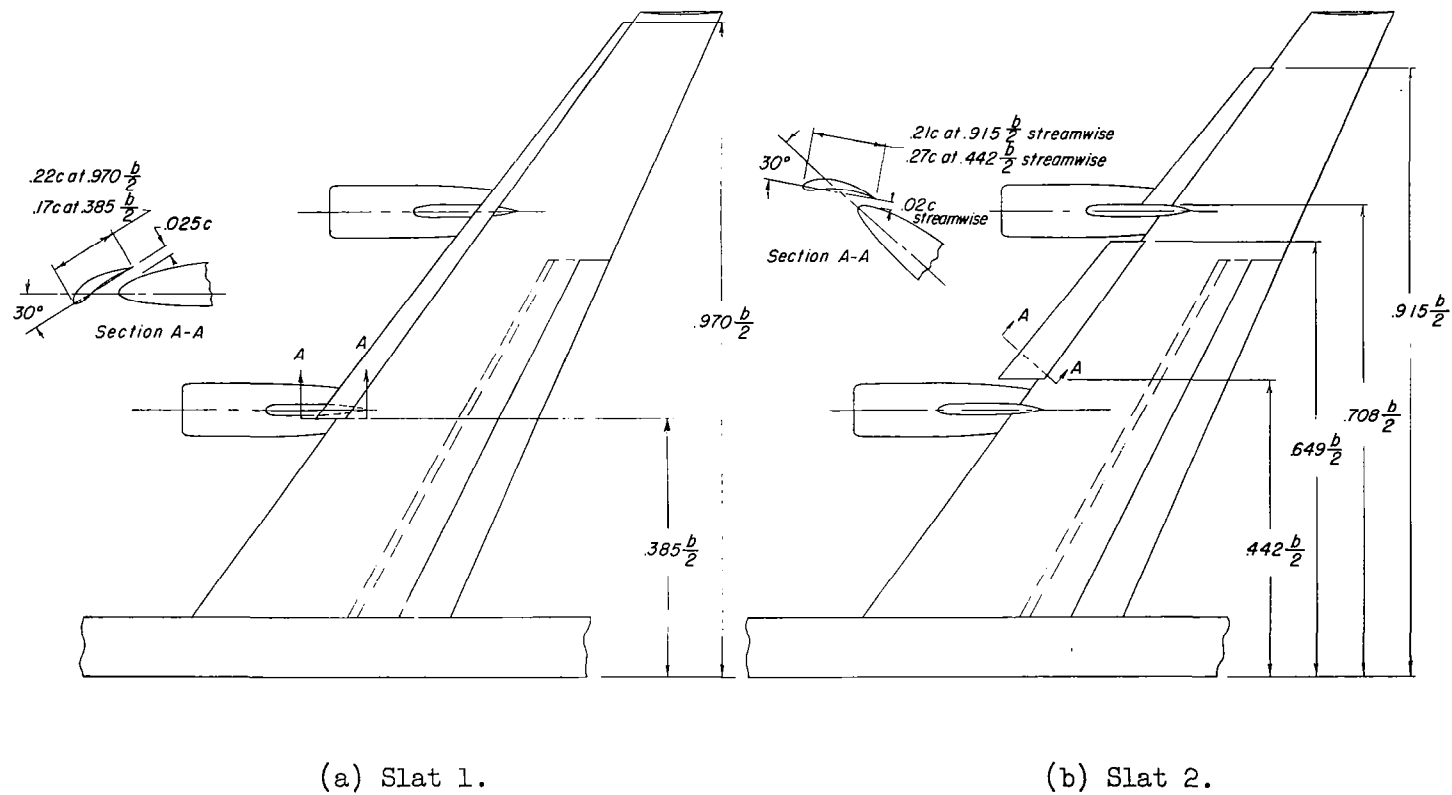
Figure 4.- Details of leading-edge slat.

0.800c

0.812c

0.015c

Pivot point

.695c

0.036c

0.6 wing thickness
at 0.800c

(a) Basic double slotted flap.

Vane

Flap

(b) Slot reduced by extending
vane trailing edge.

(c) Slot reduced by moving
flap forward.
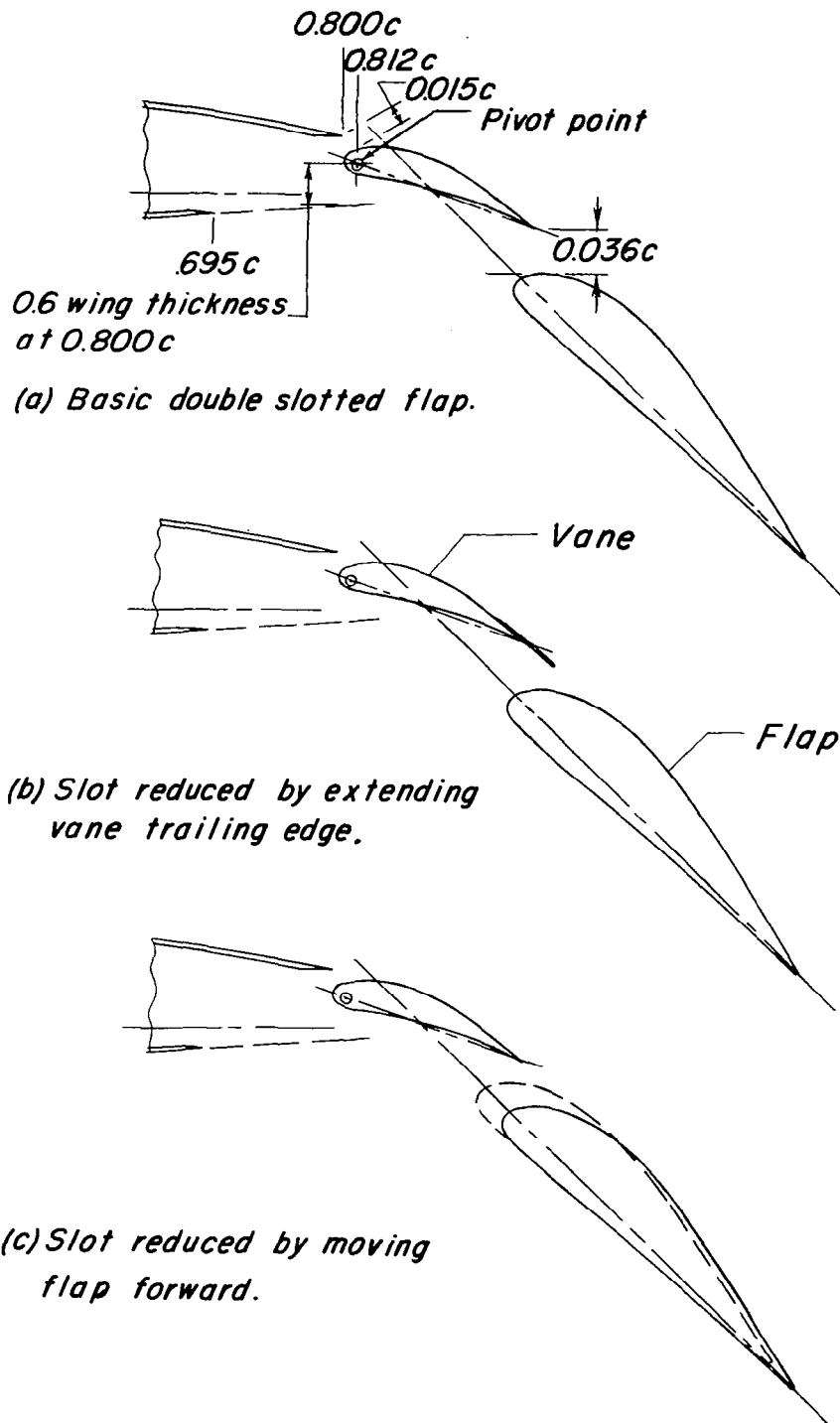
Figure 5.- Double slotted flaps tested.
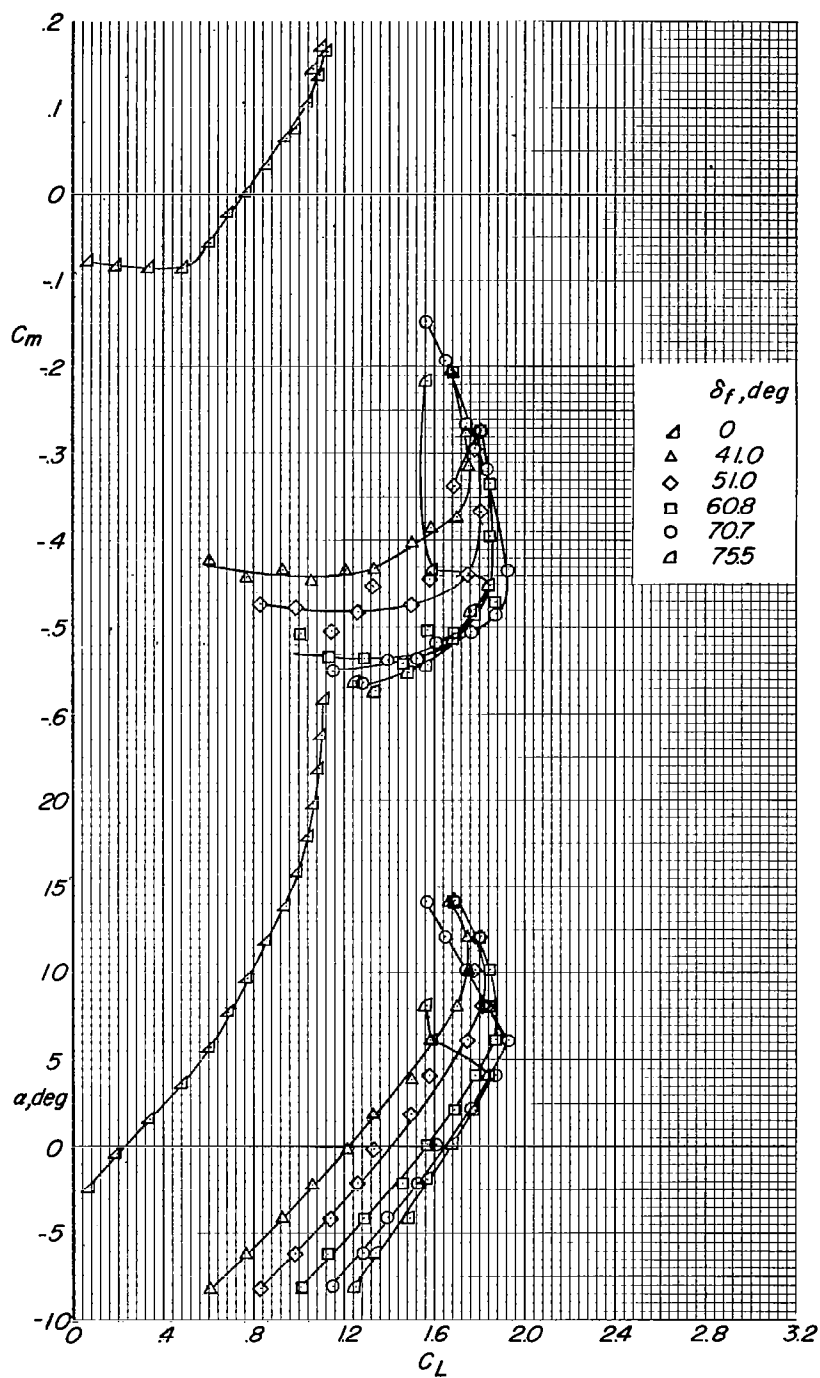
(a) C_m and α plotted against C_L.

Figure 6.- Effect of flap deflection with basic wing and fuselage.
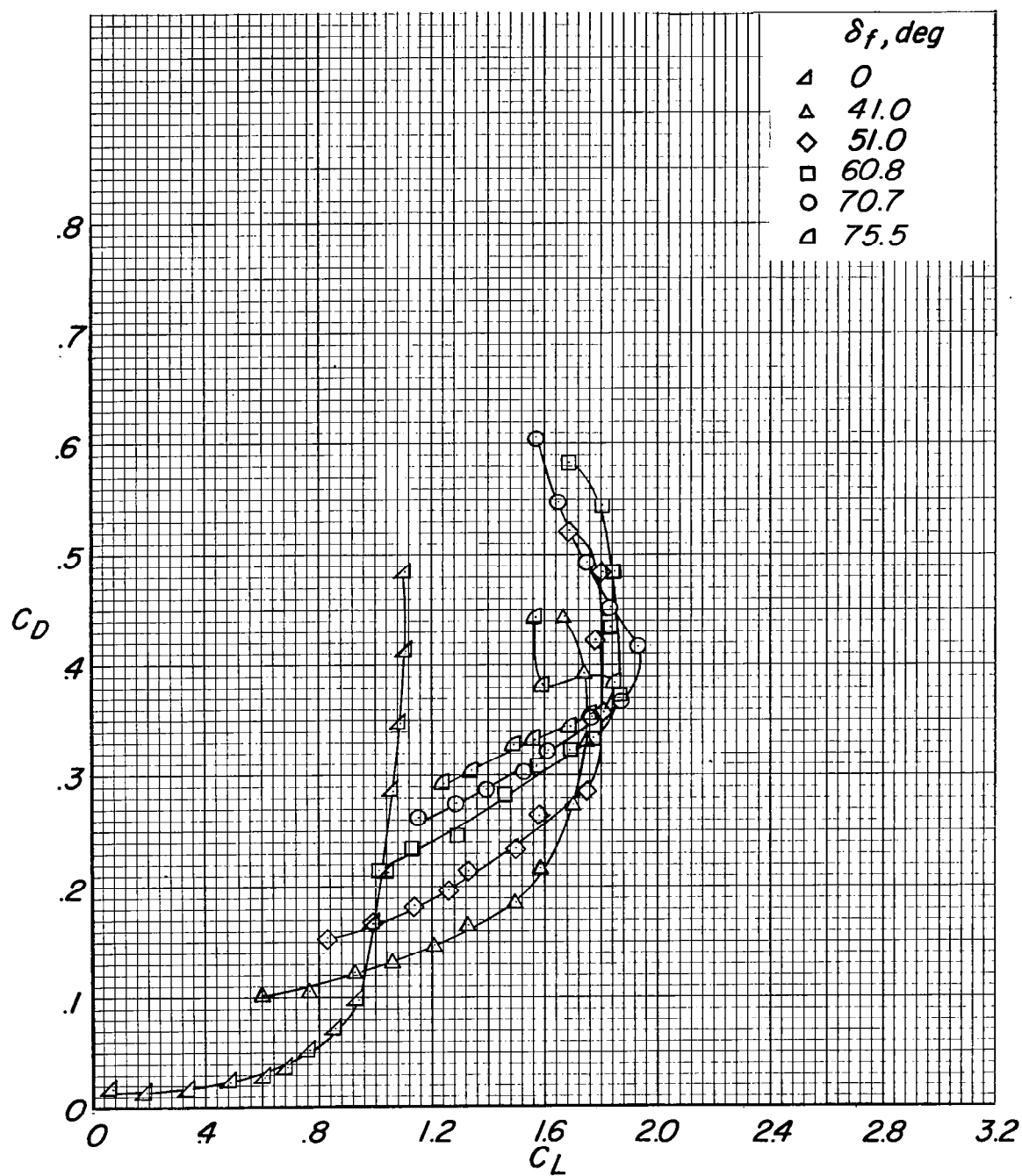
(b) C_D plotted against C_L.

Figure 6.- Concluded.
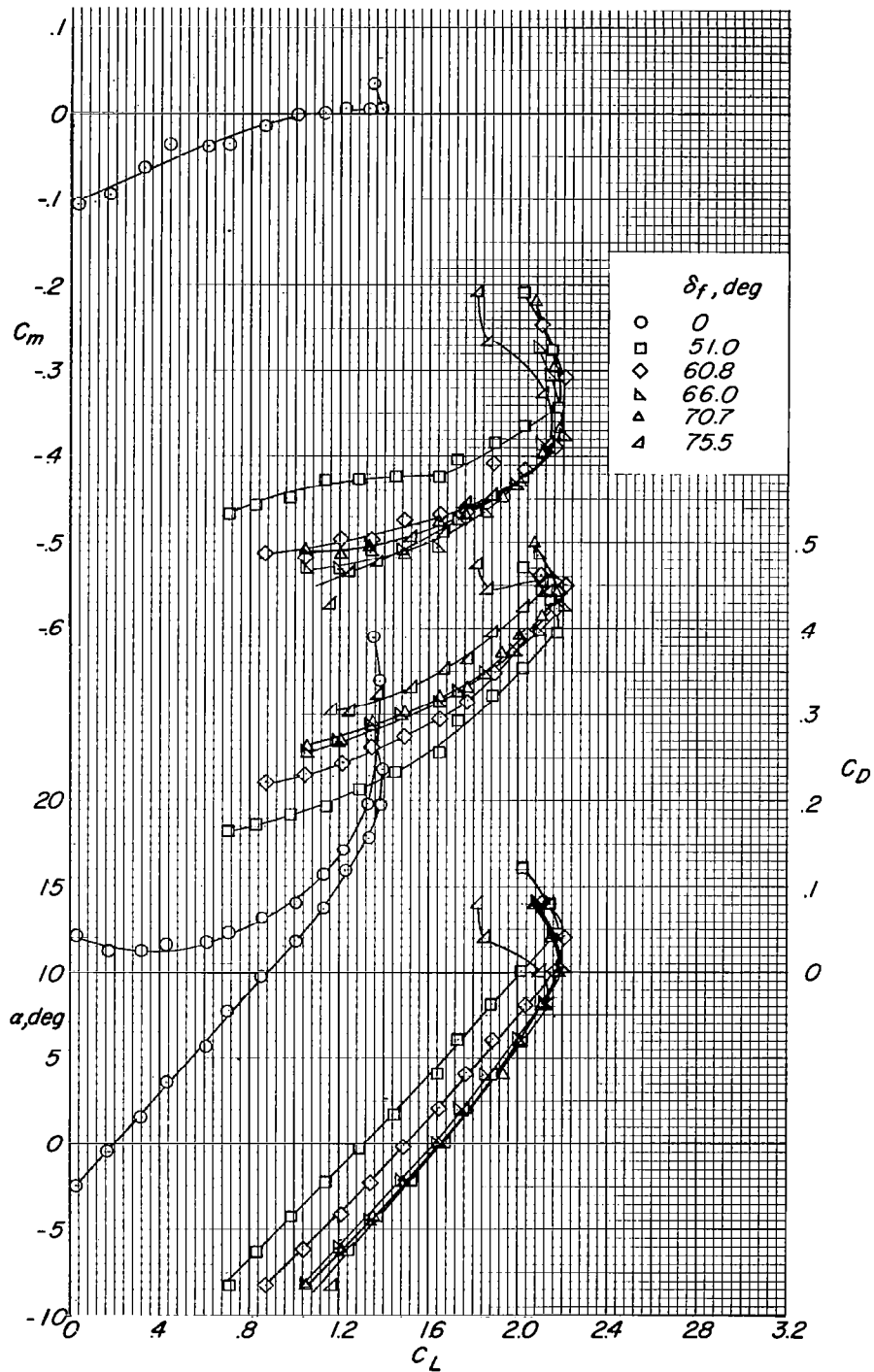
Figure 7.- Effect of flap deflection. Slat 1; nacelles open.
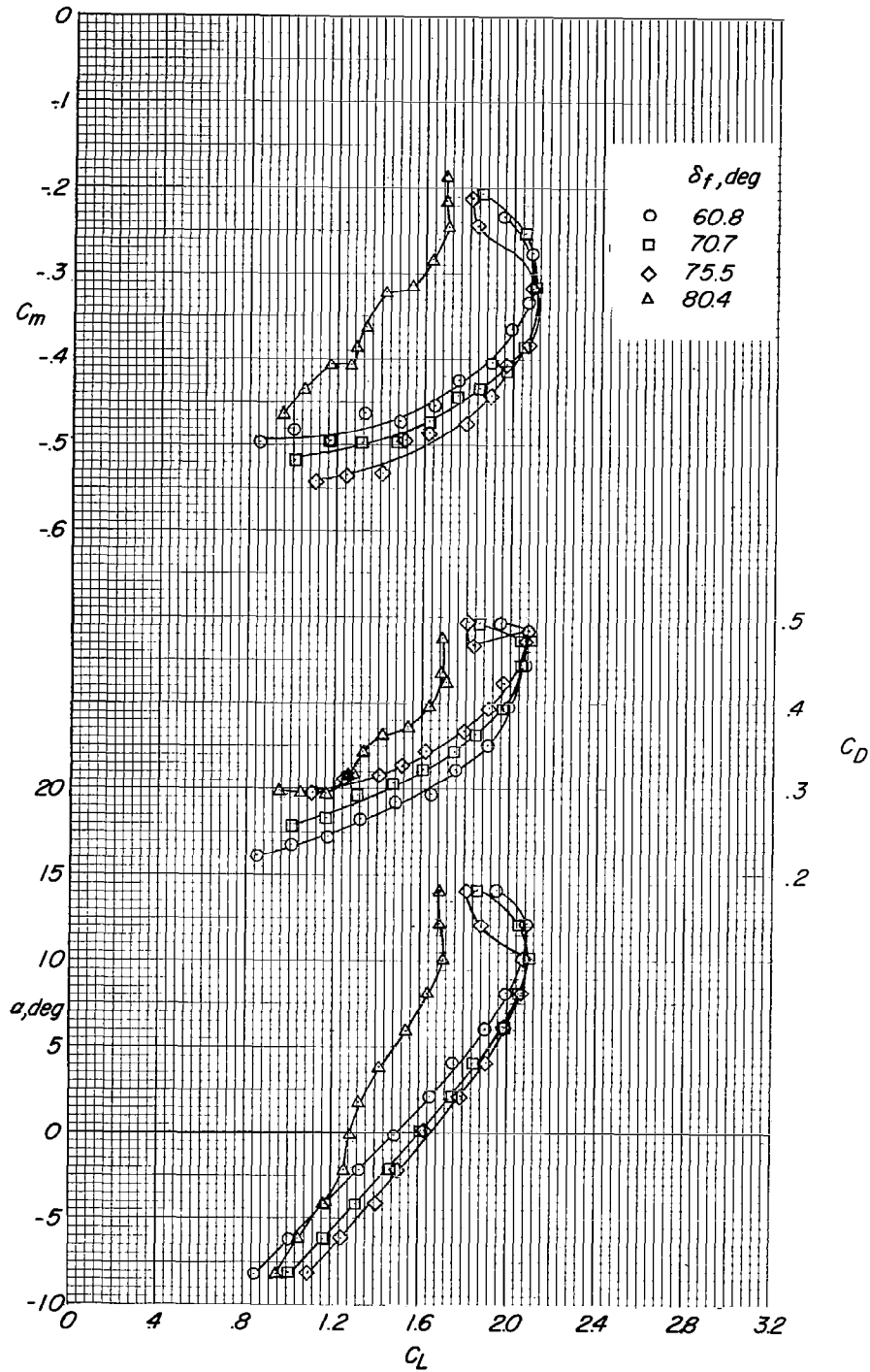
Figure 8.- Effect of flap deflection. Slat 2; nacelles plugged.
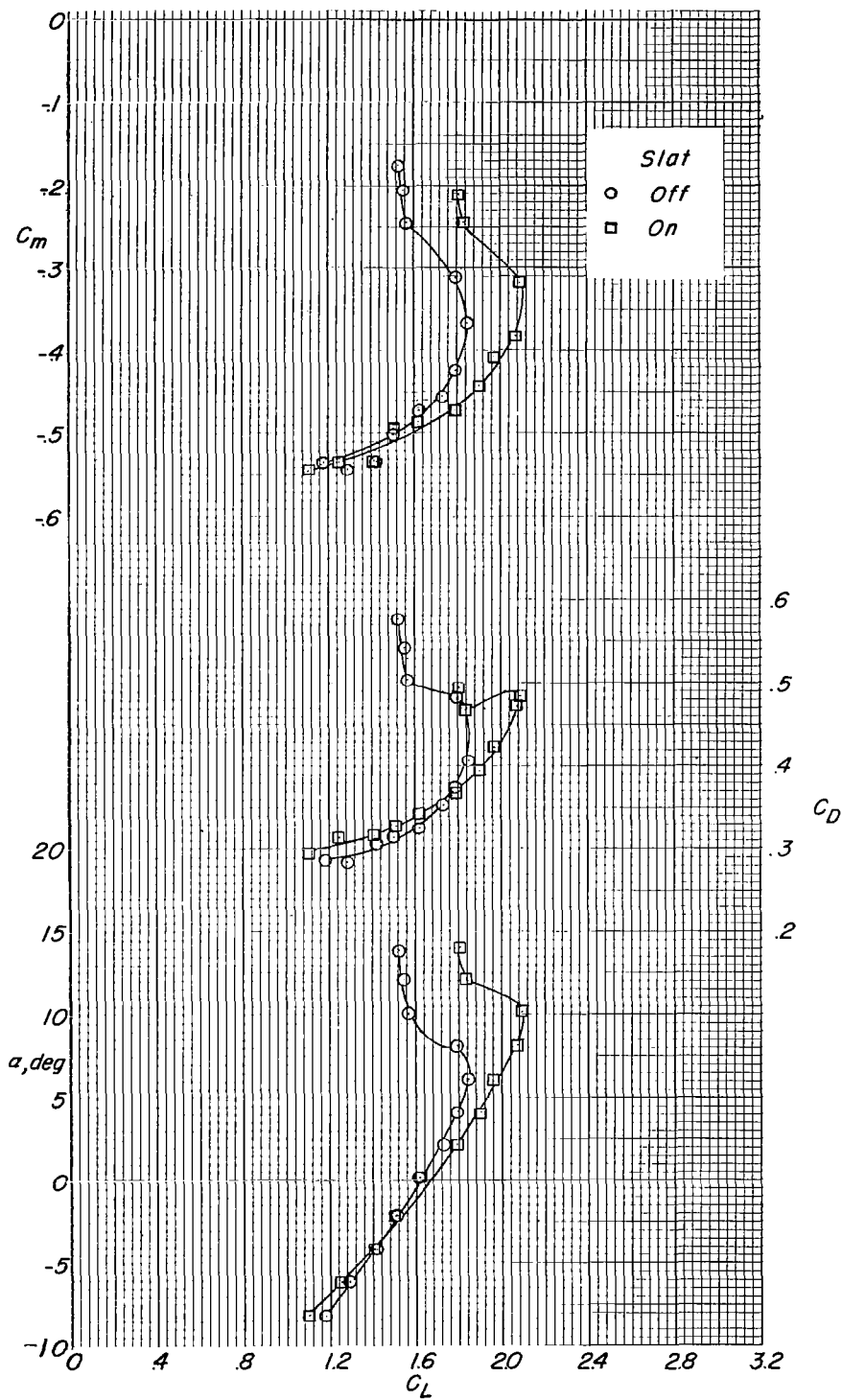
Figure 9.- Effect of slat 2. Nacelles plugged; $\delta_f = 75.5^o$.
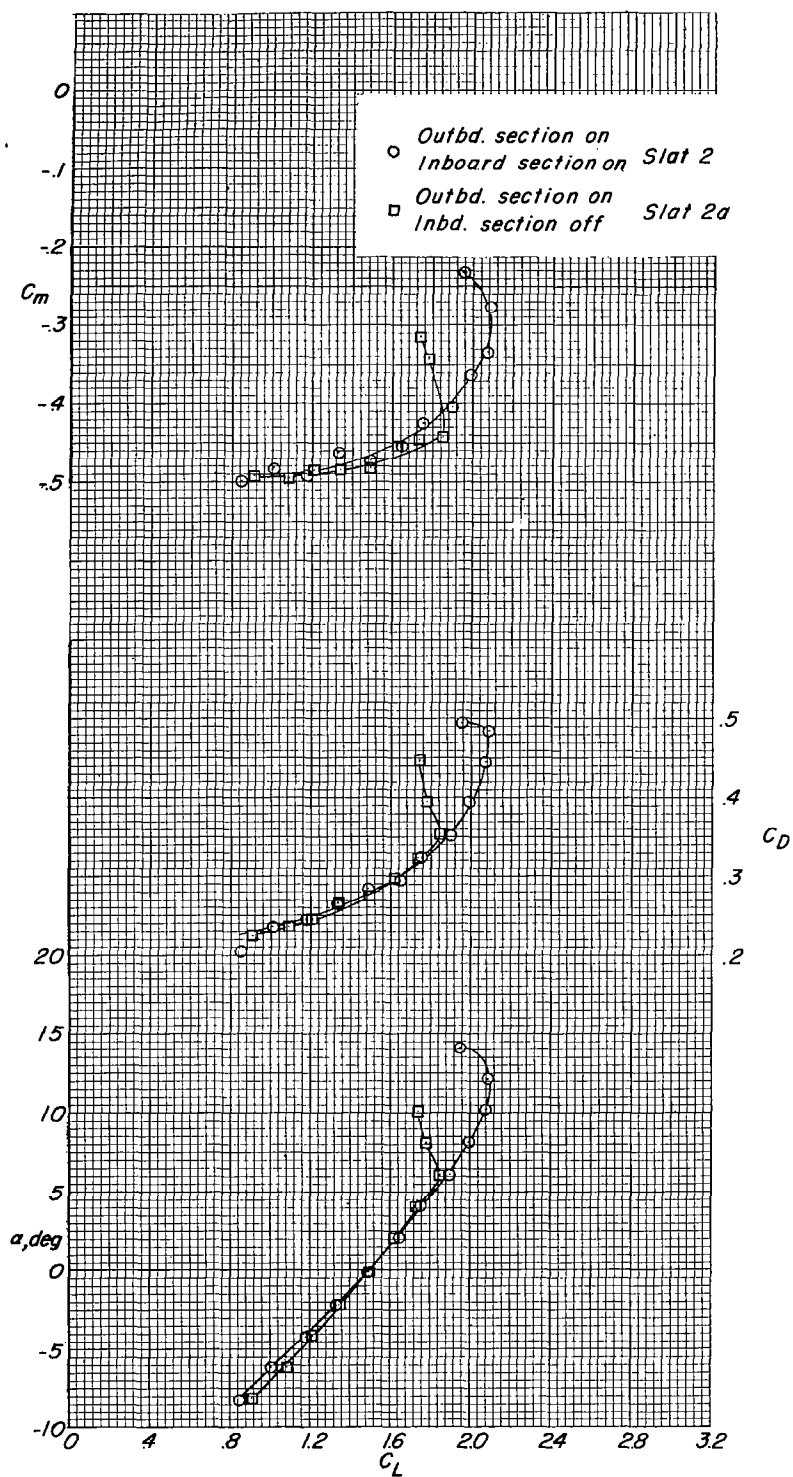
Figure 10.- Effect of slat 2 span. Nacelles plugged; $\delta_f = 60.8^\circ$.
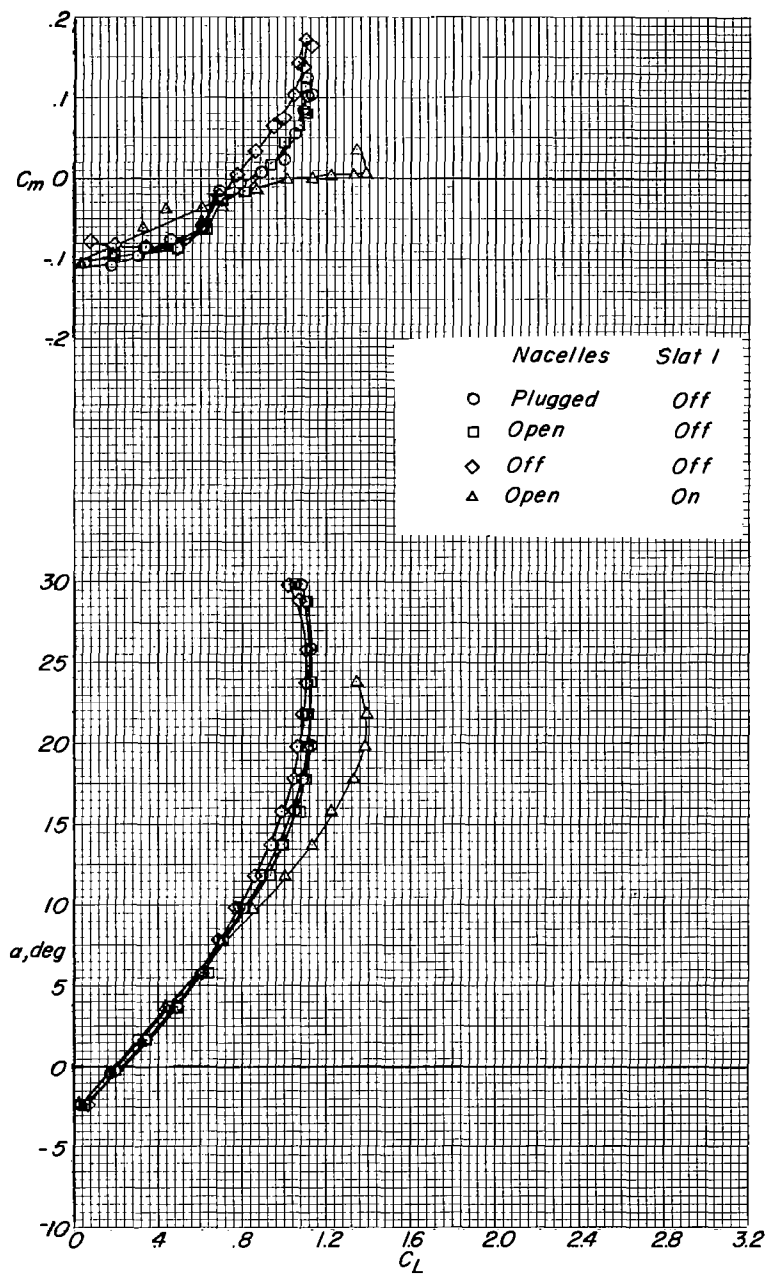
(a) C_m and α plotted against C_L.

Figure 11.- Effect of nacelles and slats. $\delta_f = 0^\circ$.

	Nacelles	Slat 1
o	Plugged	Off
□	Open	Off
◇	Off	Off
△	Open	On
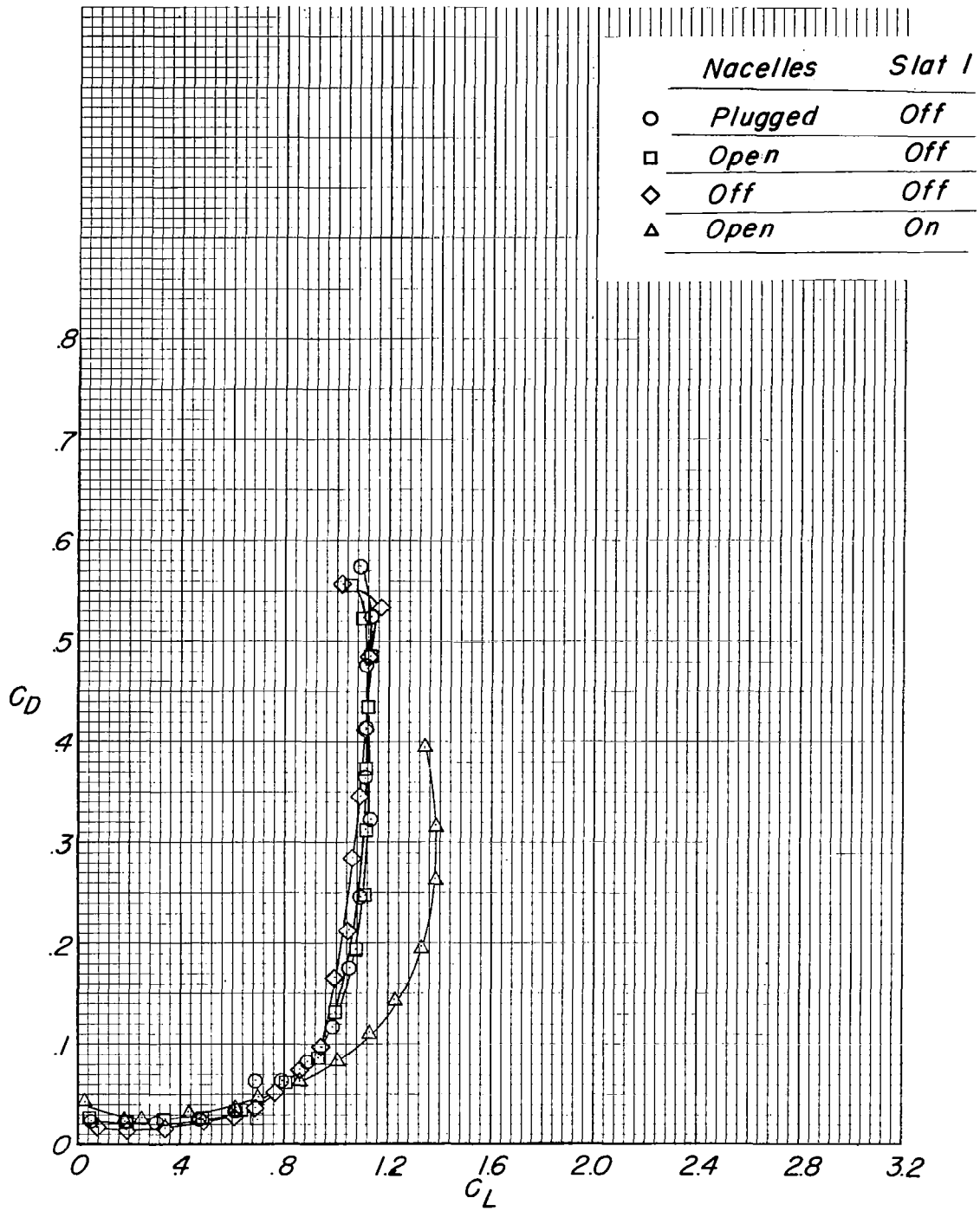
(b) C_D plotted against C_L.

Figure 11.- Concluded.
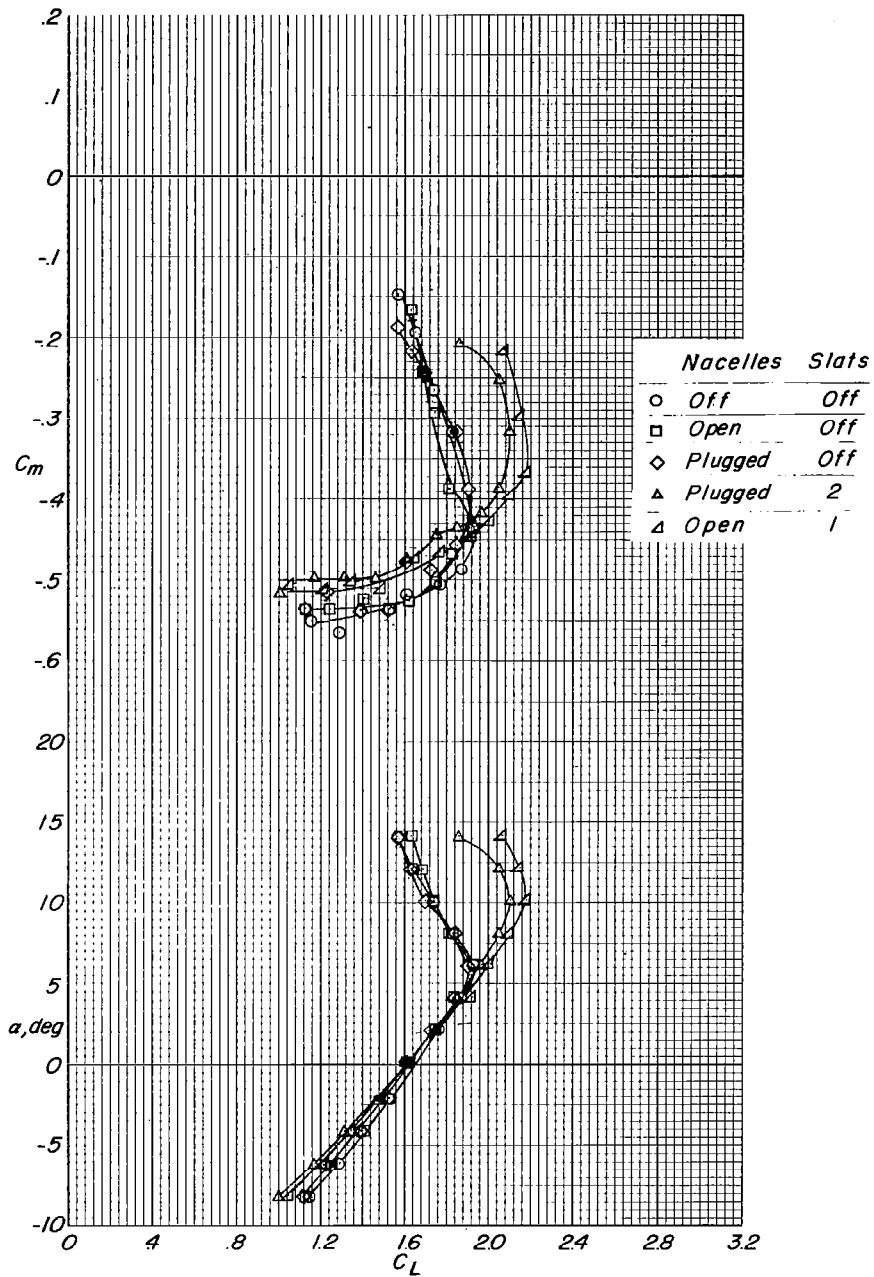
(a) C_m and α plotted against C_L.

Figure 12.- Effect of nacelles and slats. $\delta_f = 70.7^\circ$.
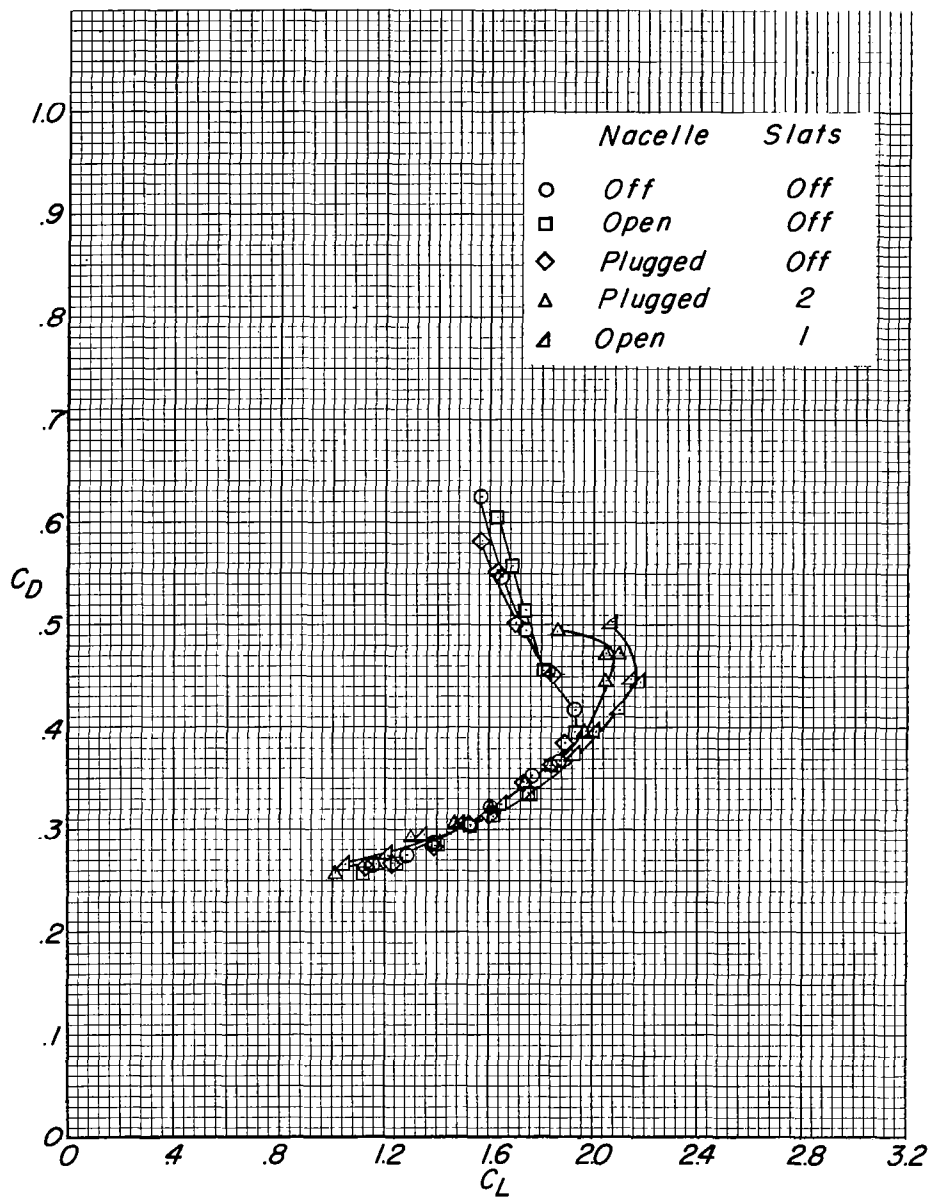
(b) C_D plotted against C_L.

Figure 12.- Concluded.
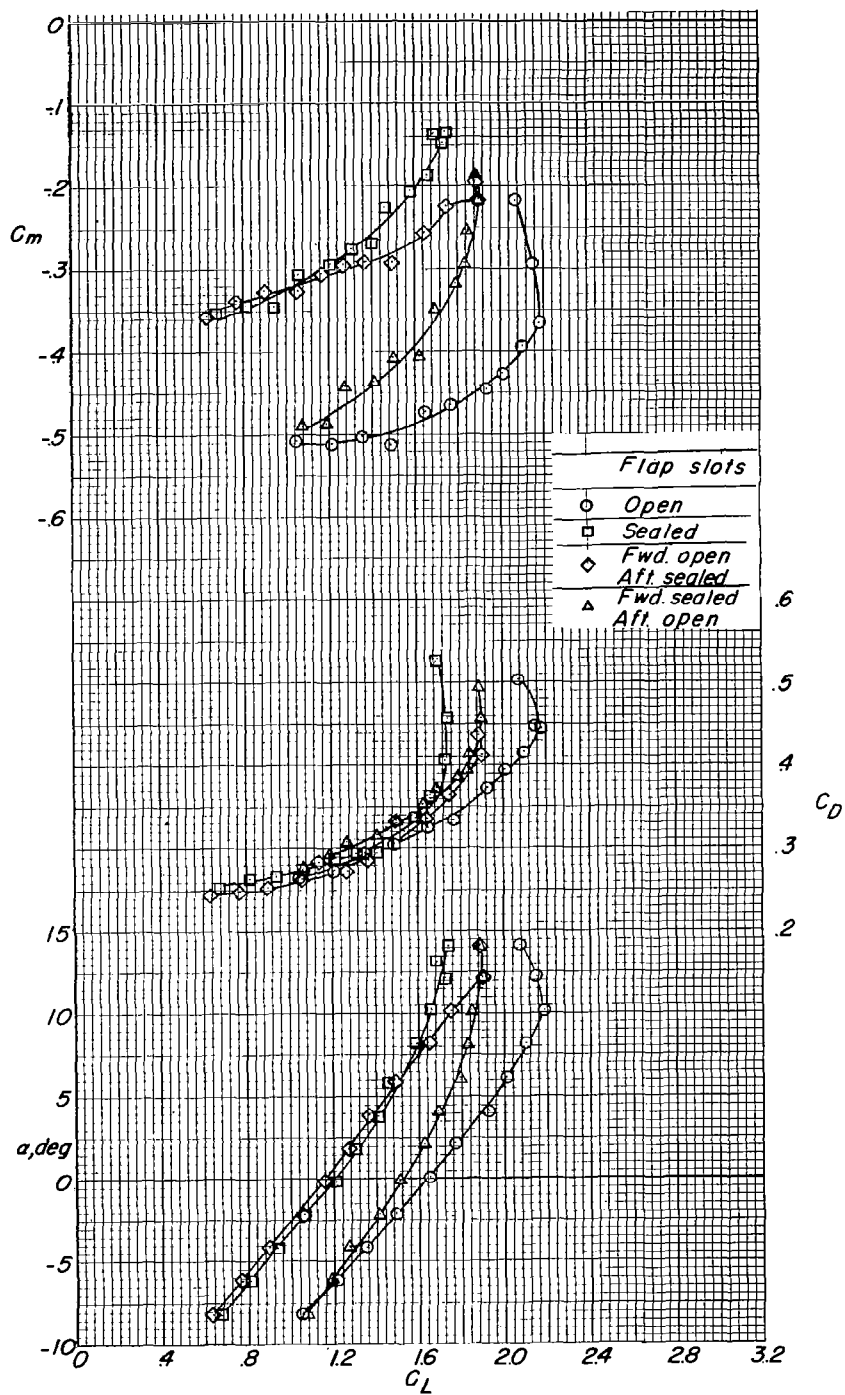
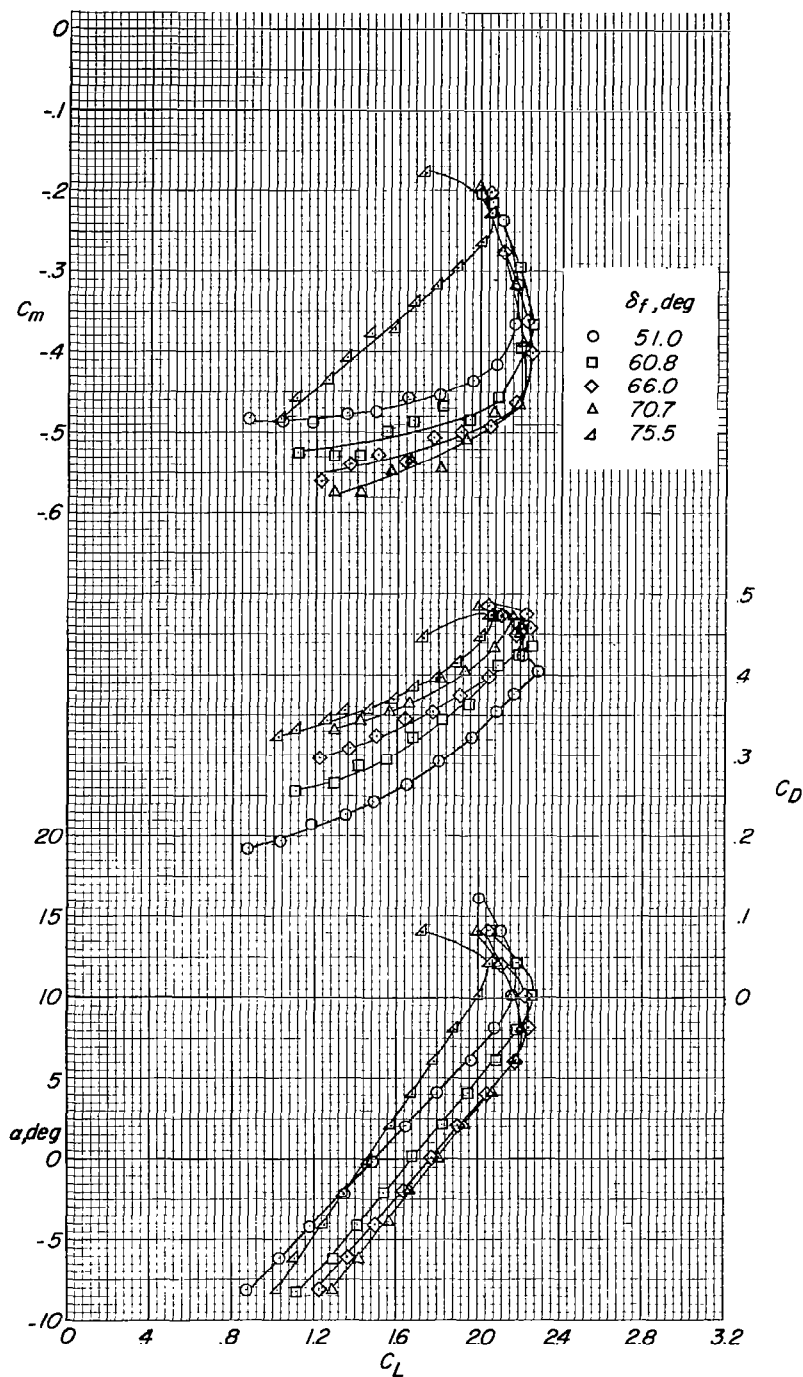Figure 13.- Effect of sealing slots. Slat 1; nacelles open; $\delta_f = 70.7^\circ$.

Figure 14.- Effect of flap deflection with trailing edge of vane chord extended to reduce flap slot about 50 percent. Slat 1; nacelles open.
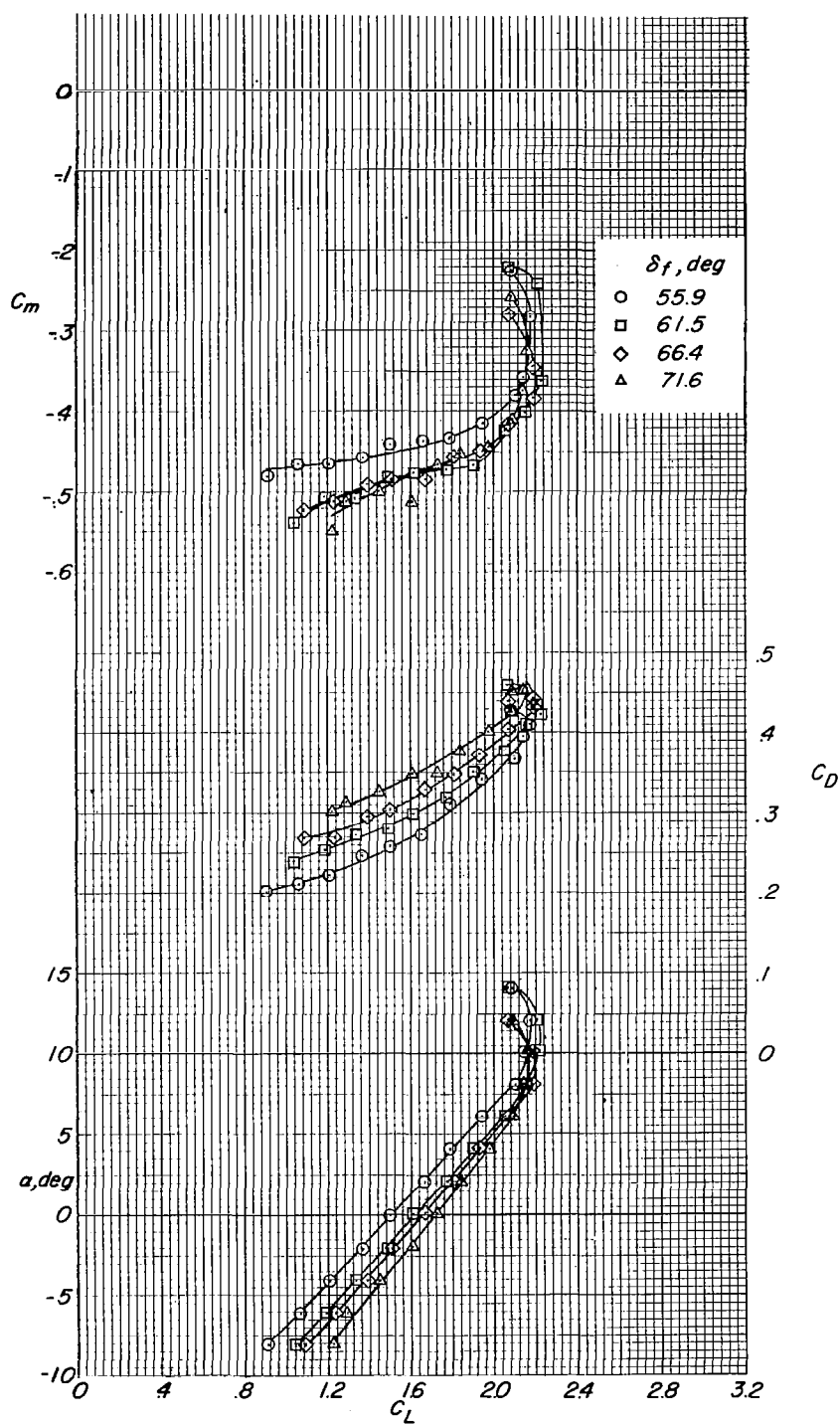
Figure 15.- Effect of flap deflection with main flap moved forward to reduce flap gap about 50 percent. Slat 1; nacelles open.
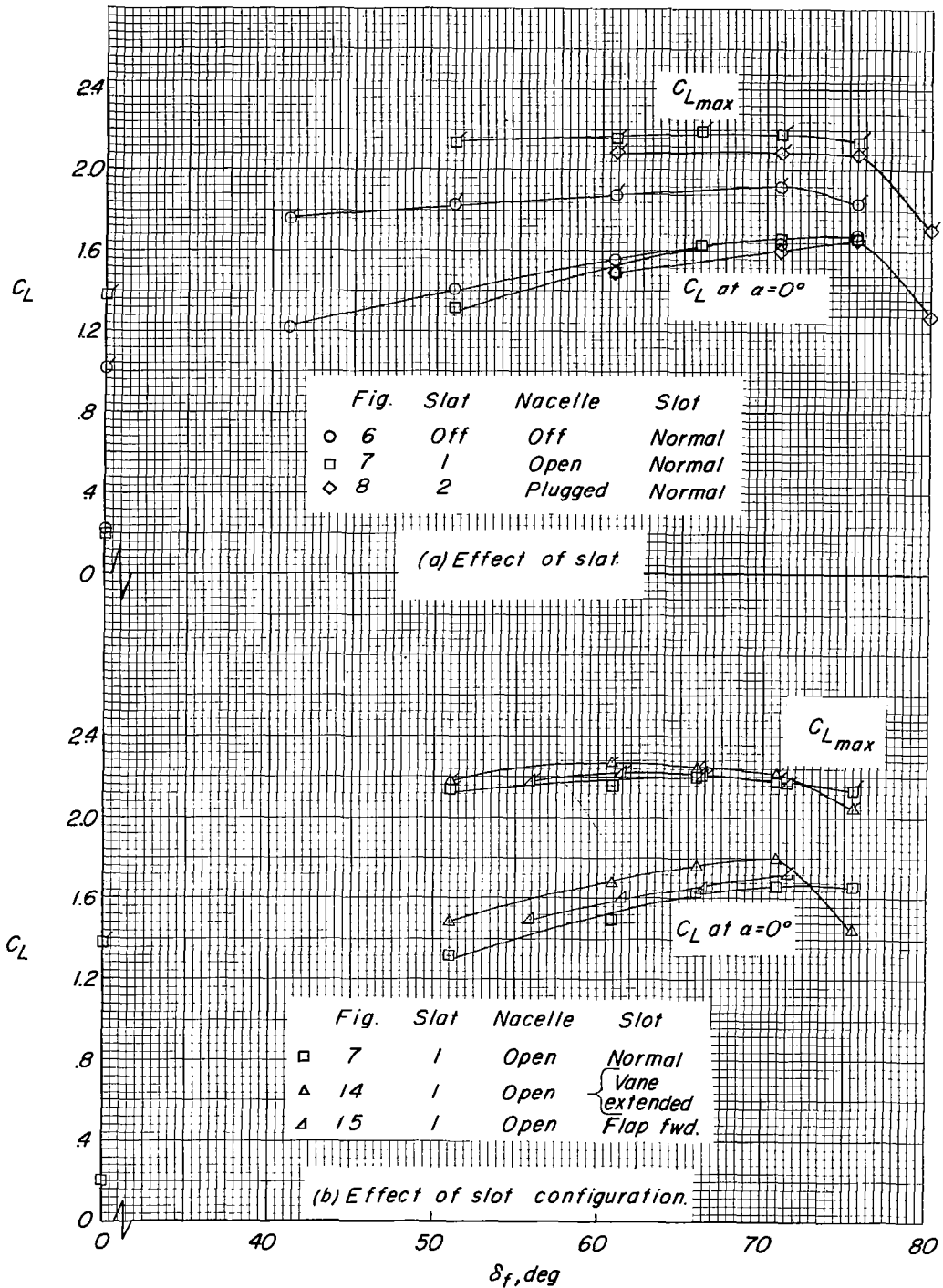
32

Figure 16.- Variation of C_L at $\alpha = 0^O$ and at α for $C_{L_{max}}$ with deflection of double slotted flaps.
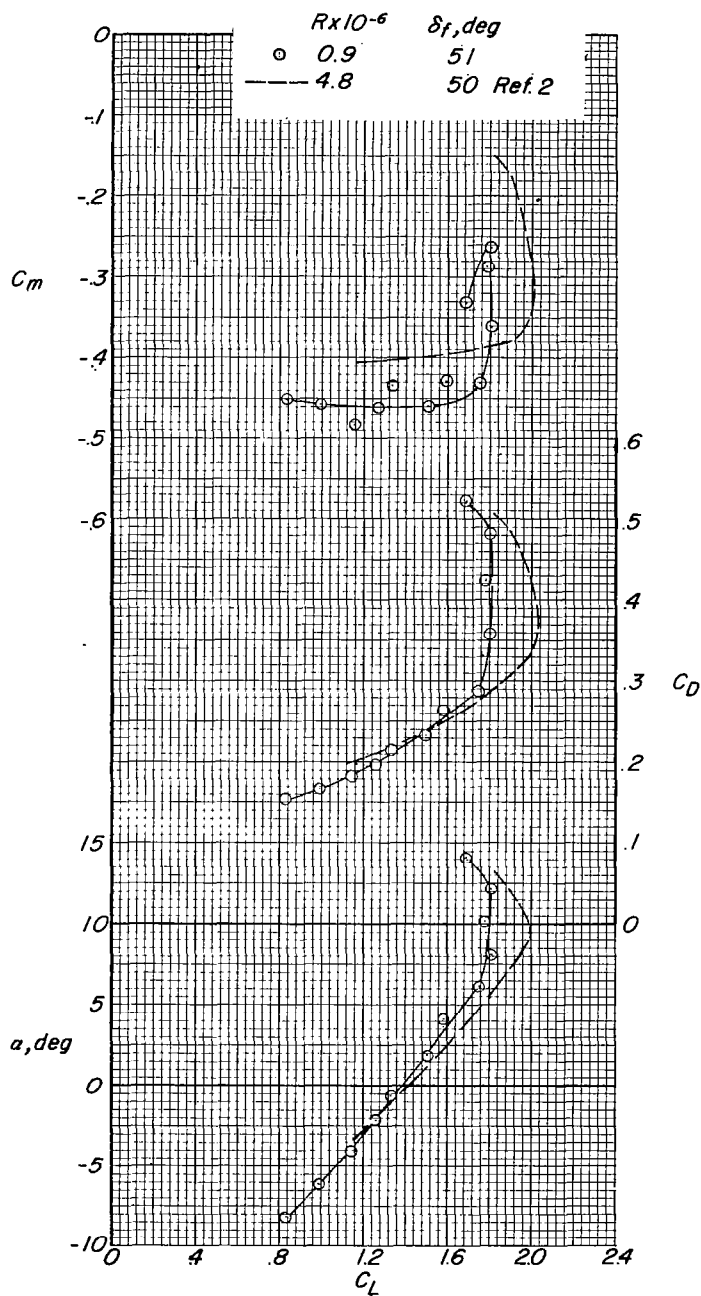
Figure 17.- Effect of Reynolds number on the aerodynamic characteristics of a 35° sweptback wing and fuselage. Center of moments is located longitudinally at 0.30c̄ (fig. 2) and vertically at 0.08c̄ above the wing root chord.

COMMANDER   T. N. D-103
ATT. SBNE, WEAPONS ENGINEERING DIV.
D LSM
NORTON AIR FORCE BASE,CALIFORNIA
                                        X
2,17-19, 2 , 2 , 2 , 3 , 44,37-39,47,48,
50-5 , *** COPIES C.I.P.A.